## Title
Desmosomal junctions are necessary for adult sinus node function



## Journal
Cardiovascular Research, 111(3)

## ISSN
1015-5007

## Authors
Mezzano, Valeria
Liang, Yan
Wright, Adam T
et al.

## Publication Date
2016-08-01

## DOI
10.1093/cvr/cvw083

Peer reviewed

Cardiovascular Research (2016) **111**, 274–286
doi:10.1093/cvr/cvw083

# Desmosomal junctions are necessary for adult sinus node function

**Valeria Mezzano[1†], Yan Liang[1†], Adam T. Wright[2], Robert C. Lyon[1], Emily Pfeiffer[2], Michael Y. Song[3], Yusu Gu[1], Nancy D. Dalton[1], Melvin Scheinman[4], Kirk L. Peterson[1], Sylvia M. Evans[5], Steven Fowler[6], Marina Cerrone[6], Andrew D. McCulloch[1,2], and Farah Sheikh[1*]**

[1]Department of Medicine, University of California-San Diego, 9500 Gilman Drive, La Jolla, CA 92093-0613C, USA; [2]Department of Bioengineering, University of California-San Diego, La Jolla, CA 92093, USA; [3]Scripps Translational Science Institute, Department of Medicine, Scripps Green Hospital, La Jolla, CA 92037, USA; [4]Department of Cardiac Electrophysiology, University of California-San Francisco, San Francisco, CA 94143, USA; [5]Skaggs School of Pharmacy, University of California-San Diego, La Jolla, CA 92093, USA; and [6]Cardiovascular Genetics Program, New York University School of Medicine, New York, NY 10016, USA

*Received 24 April 2015; revised 11 March 2016; accepted 8 April 2016; online publish-ahead-of-print 20 April 2016*

**Time for primary review: 35 days**

**Aims** Current mechanisms driving cardiac pacemaker function have focused on ion channel and gap junction channel function, which are essential for action potential generation and propagation between pacemaker cells. However, pacemaker cells also harbour desmosomes that structurally anchor pacemaker cells to each other in tissue, but their role in pacemaker function remains unknown.

**Methods and results** To determine the role of desmosomes in pacemaker function, we generated a novel mouse model harbouring cardiac conduction-specific ablation (csKO) of the central desmosomal protein, desmoplakin (DSP) using the Hcn4-Cre-ERT2 mouse line. Hcn4-Cre targets cells of the adult mouse sinoatrial node (SAN) and can ablate DSP expression in the adult DSP csKO SAN resulting in specific loss of desmosomal proteins and structures. Dysregulation of DSP via loss-of-function (adult DSP csKO mice) and mutation (clinical case of a patient harbouring a pathogenic DSP variant) in mice and man, respectively, revealed that desmosomal dysregulation is associated with a primary phenotype of increased sinus pauses/dysfunction in the absence of cardiomyopathy. Underlying defects in beat-to-beat regulation were also observed in DSP csKO mice *in vivo* and intact atria *ex vivo*. DSP csKO SAN exhibited migrating lead pacemaker sites associated with connexin 45 loss. *In vitro* studies exploiting ventricular cardiomyocytes that harbour DSP loss and concurrent early connexin loss phenocopied the loss of beat-to-beat regulation observed in DSP csKO mice and atria, extending the importance of DSP-associated mechanisms in driving beat-to-beat regulation of working cardiomyocytes.

**Conclusion** We provide evidence of a mechanism that implicates an essential role for desmosomes in cardiac pacemaker function, which has broad implications in better understanding mechanisms underlying beat-to-beat regulation as well as sinus node disease and dysfunction.

**Keywords** Desmosome • Sinus node dysfunction • Physiology/function • Arrhythmia (mechanisms) • Heart rate variability

## 1. Introduction

The heartbeat is initiated by synchronous depolarization of a network of pacemaker cells in the sinoatrial node (SAN).[1] This large heterogeneous structure is composed of thousands of pacemaker cells, each with the ability to generate action potentials spontaneously and, presumably, at different frequencies.[1,2] A regular heart rate is therefore the result of pacemaker cells attaining synchronous depolarization through mutual entrainment.[2] Current understanding of cardiac pacemaker function has primarily focused on ion channel and gap junction channel function, which are essential for generating and propagating action potentials across pacemaker cells.[3–6] Inherent to the SAN,

* Corresponding author. Tel: +1 858 246 0754; fax: +1 858 822 1355, E-mail: fasheikh@ucsd.edu

† These authors contributed equally to this work and should be regarded as joint first authors.

architecture is also anchoring junctions that structurally tether the cell–cell interface of adjacent pacemaker cells;[7] however, their role in SAN function remains unknown.

Desmosomes are a subset of anchoring junctions that link the intermediate filament cytoskeleton between two adjacent cells.[8] They are formed by specialized desmosomal cadherins (desmoglein and desmocollin) from two adjacent cells that link to each other in the extracellular space, which then intracellularly link to the intermediate filament (i.e. desmin) through desmoplakin's (DSP) interaction with plakoglobin and plakophilin.[8] DSP is necessary for desmosomal assembly.[9] In ventricular muscle, desmosomes provide mechanical stability to cardiomyocytes, but recent insights also suggest their potential importance in gap junction[10,11] and ion channel function.[12,13] Recent ultrastructural studies also describe their abundance in the SAN; however, the unique cellular heterogeneity (smaller central vs. larger periphery cells), cytoskeletal and junctional architecture, as well as electrophysiological properties of the SAN present as being distinct from ventricular cardiomyocytes.[1,3–7] The SAN also possesses a rudimentary contractile apparatus, unlike ventricular cardiomyocytes.[7] To support the prominent cytoskeletal architecture of ventricular cardiomyocytes, they contain additional composite junctions (mix of desmosomal and fascia adherens junction proteins),[7,14] which have not been reported in SAN cells, suggesting a potentially distinct role for desmosomes in SAN compared with ventricular cardiomyocytes. However, the physiological relevance of desmosomal anchoring junctions in the SAN, including their contribution to differences in pacemaker activity between cells from across the SAN as well as whether their disruption would impact SAN function, has not been addressed.

Through the generation of a novel cardiac conduction-specific DSP knockout mouse model (DSP csKO) as well as clinical and genetic evaluation of an adult patient with primary sinus arrhythmias, we provide evidence that desmosomes are critical for normal SAN function and mutual entrainment *in vivo*. Specifically, we show an important role for SAN in lead pacemaker cells, which showed the most vulnerability to loss of desmoplakin and disruption of desmosomes. Studies exploiting ventricular cardiomyocytes that harbour DSP loss further translate the importance of DSP-associated mechanisms in driving beating synchrony of working cardiomyocytes as they phenocopy the loss of beat-to-beat control observed in DSP csKO mice and atria. These results reveal that the establishment of a spontaneous rhythmic heart rate *in vivo* is an emergent function of a network of pacemaker cells that require desmosomes for co-ordinated function.

# 2. Methods

An expanded Methods section is provided in the Supplementary material online.

## 2.1 Generation of mouse lines

Mouse strains used included DSP floxed ($DSP^{flox/flox}$), $Hcn4^{cre\text{-}ERT2}$, and $Rosa26^{TomRed}$ as published elsewhere. Cardiac conduction-specific DSP knockout mice were generated by crossing $DSP^{flox/flox}$ mice with $Hcn4^{cre\text{-}ERT2}$ mice. Tamoxifen injection was performed to achieve conduction-specific ablation of DSP in mice using previously published protocols. For lineage tracing studies, $DSP^{flox/flox}$:$Hcn4^{cre\text{-}ERT2}$ mice were crossed with $Rosa26^{TomRed}$ mice. For experimental studies, adult mice were sacrificed by cervical dislocation following anaesthesia by intraperitoneal injection of a mixture of ketamine (100 mg/kg) and xylazine (5 mg/kg), while the depth of anaesthesia was monitored by toe pinch. Neonatal mice were sacrificed by decapitation. All animal procedures were in full compliance with the guidelines approved by the University of California-San Diego Animal Care and Use Committee and carried out in accordance with the Guide for the Care and Use of Laboratory Animals of the National Institutes of Health.

## 2.2 Electron microscopy

Fixed hearts were excised, and only the cardiac region encompassing the junction of the superior caval vein (SCV) and right atrium was processed for EM as previously described.[15]

## 2.3 Whole mount imaging

Hearts were fixed with 4% paraformaldehyde/PBS solution overnight at 4°C and placed on Sylgard-®184 (Dow Corning) coated petri dishes for imaging. Bright field and epifluorescence images were acquired with an Olympus MVX10® MacroView microscope.

## 2.4 Pacemaker cell isolation

Pacemaker cells were isolated from hearts of tamoxifen-treated adult DSP TomRed reporter mice as previously described,[16] with minor modifications.

## 2.5 IF microscopy

Cells were stained with primary antibodies against desmoplakin (mouse, 1:100, AbDSerotec), desmin (rabbit, 1:100, Santa Cruz Biotechnology), plakoglobin (goat, 1:100, Santa Cruz Biotechnology), and/or α-actinin (mouse, 1:100, Sigma) and imaged as previously described.[10]

## 2.6 Protein blot analysis

Total protein was isolated using methods as previously described.[6] Immunodetection of desmoplakin (mouse, 1:1000, AbDSerotec), plakophilin-2 (mouse, 1:100, Fitzgerald), plakoglobin (goat, 1:1000, sigma), desmoglein-2 (mouse, 1:100, Fitzgerald), desmocollin-2 (mouse, 1:500, Fitzgerald), N-cadherin (rabbit, 1:100, Abcam), hyperpolarization activated cyclic nucleotide-gated potassium channel 4 (rat, 1:1000, Abcam), connexin 45 (rabbit, 1:1000, Invitrogen), connexin 43 (rabbit, 1:10000, Sigma), connexin 30.2 (rabbit, 1:500, Abcam), and glyceraldehyde 3-phosphate dehydrogenase (mouse, 1:2000, Santa Cruz Biotechnology) was performed as previously described.[10]

## 2.7 ECG telemetry recordings and interbeat interval variability analyses in mice

Conscious ECG telemetry using an implantable wireless transmitter/receiver system (Data Sciences International/Ponemah) was performed in mice as previously described.[17] Sinus pause analysis was performed on LabChart® (ADInstruments) by manual inspection of ECG telemetry traces blinded to the group. Interbeat interval variability analyses were performed on LabChart® (ADInstruments). Twenty minutes of recorded telemetry ECGs were analysed using the heart rate variability module.

## 2.8 Clinical and genetic evaluation of a patient presenting with sinus arrhythmias

The patient was referred to the Cardiovascular Genetics Program at New York University (NYU) School of Medicine for a second opinion upon discovery of frequent ectopic beats and sinus bradycardia. The patient underwent comprehensive clinical evaluation by undergoing cardiac MRI, an electrophysiological study, and implantation of a loop monitor (Linq, Medtronic) without complications. A comprehensive genetic screen of 77 cardiomyopathy-associated genes was performed on DNA extracted from peripheral blood by a commercial laboratory (GeneDx, Gettysburg, Maryland) using next-generation sequencing. Eventual findings were re-confirmed by capillary sequencing. This clinical study was approved by the institutional ethics review board of the NYU School of Medicine (09-0297) and conforms to the principles in the Declaration of Helsinki. Informed consent was obtained for the inclusion of patient data.

### 2.9 Interbeat interval variability and SAN functional analyses in isolated mouse atria

Mouse atrial preparations were isolated as previously described,[5] with minor modifications. Two platinum recording electrodes were placed on the right atrium to measure baseline electrograms. Recordings were performed at 5000 Hz in LabVIEW. Baseline electrograms (10–20 s) were acquired when the beating rate had stabilized. The fluorescent potentiometric dye di-4-ANEPPS 20 μM (Invitrogen®, CA) was loaded after the baseline electrogram was recorded. The preparation was excited with a light-emitting diode array (LEDtronics) at 470 nm. Fluorescence was collected by a custom tandem lens optical macroscope, filtered with a longpass 610 nm filter, and collected with a high speed 14-bit CMOS camera (MiCAM Ultima L, SciMedia) at 1000 frames per second and a spatial resolution of 100 × 100 pixels at 0.1 × 0.1 mm per pixel. Data were analysed using LabChart® software (ADInstruments).

### 2.10 Interbeat interval variability analyses in neonatal mouse cardiomyocyte cultures

Neonatal ventricular cardiac myocytes isolated from $Dsp^{flox/flox}$ mice were plated on laminin-coated petri dishes and infected with AdLacZ and AdCre, as previously described.[10] Spontaneous electrical activation was detected in cardiomyocytes using the voltage-sensitive fluorescent dye di-8-ANEPPS (Life Technologies). Dye was loaded in a solution of 0.1% Pluronic F-127 and 30 μM di-8-ANEPPS in antibiotic-free media for 25 min, before switching to antibiotic- and serum-free media for imaging. Data were analysed using LabChart® software (ADInstruments). Optical data were analysed with custom software in MATLAB.

### 2.11 Statistical analysis

Statistical analyses were performed on GraphPad Prism (GraphPad Software Inc.). Data presented in the text and figures are expressed as mean values ± SEM. Significance was evaluated by Student's *t*-test. A *P*-value of $<0.05$ was considered statistically significant.

## 3. Results

### 3.1 Desmosomal structures in the adult mouse pacemaker complex

Previous studies have identified desmosomal structures and proteins in the pacemaker complex (PC) of species such as the monkey and guinea pig;[18,19] however, they have not been specifically evaluated in the mouse PC (*Figure 1A*). Representative electron micrographs highlight heterogeneity of cell types within the adult mouse PC (*Figure 1B*), compared with cells of the atrial myocardium, which show a more homogenous population of atrial cardiomyocytes (*Figure 1C*). SAN pacemaker cells could be identified by their high mitochondrial and glycogen content along with their sparse contractile apparatus (*Figure 1B*), as similarly described in other species.[20] This is in contrast to atrial cardiomyocytes, which contain abundant tightly organized sarcomeres (*Figure 1C*). Representative micrographs also revealed desmosomes between pacemaker cells (*Figure 1D*), which were similarly observed between atrial cardiomyocytes (*Figure 1E*). Fascia adherens anchoring junctions could also be identified between pacemaker cells (*Figure 1D*), but they did not display the typical ribbon-like extensions found in atrial cardiomyocytes (*Figure 1E*). Gap junctions were identified between pacemaker cells; however, they appeared sparse and shortened in length (*Figure 1D*; see Supplementary material online, *Figure S1*), as described in the rabbit and cat PC.[20,21] Gap junctions were found in close proximity to desmosomes (*Figure 1D*), suggesting a potential relationship between these structures in the PC.

### 3.2 Characterization of an adult cardiac conduction-specific DSP knockout mouse model reveals loss of identifiable desmosomes in the adult mouse PC

To determine a role for desmosomes in the adult mouse PC, we generated a novel mouse model harbouring cardiac conduction-specific ablation of the central desmosomal protein, desmoplakin (DSP csKO), using an inducible *Hcn4-Cre-ER*$^{T2}$ mouse line. DSP is a central component of the desmosomal complex that is essential for desmosomal assembly in early embryonic development and mechanical integrity of ventricular cardiomyocytes.[8,10] To determine the specificity of *Hcn4-Cre-ER*$^{T2}$ to target cardiac conduction cells in adult DSP csKO mice, we crossed $Dsp^{flox/+}$:$Hcn4^{creERT2(+)}$ mice with a Cre-inducible *R26RtdTomato* reporter mice, to generate $Dsp^{flox/+}$:$Hcn4^{creERT2(+)}$:$ROSA26^{TomRed+}$ mice. R26RtdTomato reporter mice express Tomato Red (TomRed) when exposed to Cre recombinase. Thus, TomRed expression in the background of $Dsp^{flox/+}$:$Hcn4^{creERT2(+)}$ mice genetically mark all Hcn4 positive (+) cells in this model at a time point when Cre is activated with tamoxifen injection. Since the mice were injected at 1 month of age, TomRed would thus mark all cells within the adult heart expressing Hcn4. Macroscopic analyses of adult $Dsp^{flox/+}$:$Hcn4^{creERT2(+)}$:$ROSA26^{TomRed+}$ mouse hearts revealed that Hcn4-Cre targeted cells of the adult mouse SAN (*Figure 2*). Anterior views showed TomRed activity localized to the junction of the SCV adjacent to the right atrium, consistent with the localization of the compact node (*Figure 2B* and *D*). Posterior views highlighted TomRed activity extending from the SCV toward a mesh-like network surrounding the large coronary sinus (*Figure 2F* and *H*). Lineage tracing studies revealed that Hcn4-Cre also targeted cells of the adult atrioventricular node and His-Purkinje network (see Supplementary material online, *Figure S2*).

To determine DSP knockdown efficiency in the SAN, we assessed DSP protein localization and expression in isolated SAN cells (*Figure 3A–F*) and compact node-enriched tissue (*Figure 3G* and *H*) in adult DSP csKO hearts harbouring the TomRed reporter. IF staining analysis showed that TomRed-negative cardiomyocytes (desmin positive with no Cre recombinase activity) showed DSP localization at the cell junction and lateral ends (*Figure 3A*, *C*, and *E*; see Supplementary material online, *Figure S3*). IF staining of TomRed-positive cardiomyocytes showed the loss of DSP immunoreactivity (*Figure 3B*, *D*, and *F*; see Supplementary material online, *Figure S3*). Protein blot analyses of DSP expression in compact node-enriched tissues from adult DSP csKO ($Dsp^{flox/flox}$:$Hcn4^{creERT2(+)}$: $ROSA26^{TomRed+}$) vs. control ($Dsp^{flox/+}$:$Hcn4^{creERT2(+)}$: $ROSA26^{TomRed+}$) hearts further showed the loss of DSP protein (*Figure 3G* and *H*). DSP loss resulted in a significant reduction in desmoglein-2, desmocollin-2, and plakophilin-2 protein levels in the compact SAN node and SAN cells of DSP csKO mice compared with controls (*Figure 3H*; see Supplementary material online, *Figure S3*). Interestingly, no significant differences in the levels of fascia adherens-associated proteins, plakoglobin, and N-cadherin were observed in the compact SAN node and SAN cells of DSP csKO vs. control mice (*Figure 3H*; see Supplementary material online, *Figure S3*). Consistent with protein blot and IF microscopy analyses, representative electron micrographs from adult DSP

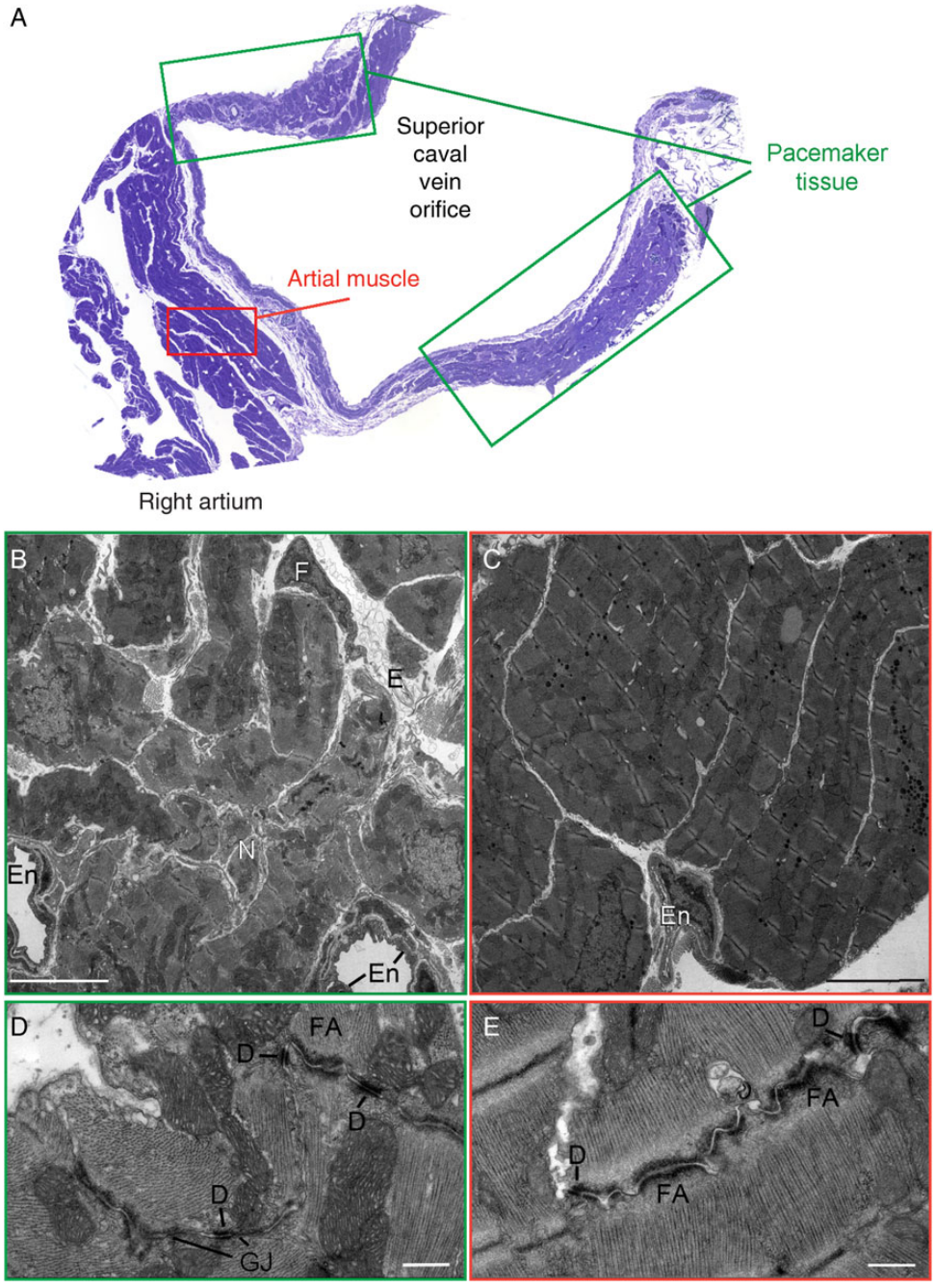


**Figure 1** Desmosomal junctions in the mouse pacemaker complex. (*A*) Representative semi-thin section of the areas used for ultrastructural analysis stained with Toluidine blue. In green boxes the areas used for pacemaker complex analysis, in red boxes working right atrial tissue areas. (*B*–*E*) Representative transmission electron micrographs from the mouse pacemaker complex (*B* and *D*) and right atrial muscle tissue (*C* and *E*). The cellular composition (*B* and *C*) and cell–cell junction structures (*D* and *E*) are highlighted in both cardiac regions ($n = 3$). E, extracellular matrix; En, endothelial cell; N, nerve bundle; F, fibroblast; D, desmosome; FA, fascia adherens junction; GJ, gap junction. Bar represents 5 μm in *B* and *C*. Bar represents 500 nm in *D* and *E*.

csKO (*Figure 3I* and *J*) and control (*Figure 3K* and *L*) PC revealed that unlike controls, in which desmosomes could be identified in abundance (*Figure 3I* and *J*), that defined desmosomal structures could not be identified in adult DSP csKO PC (*Figure 3K* and *L*). In contrast, defined desmosomes could be identified in atrial cardiomyocytes adjacent to the SAN in adult DSP csKO hearts (*Figure 3M* and *N*), underscoring the specificity of the desmosomal defects to the PC.

## 3.3 Dysregulation of DSP (loss or mutation) leads to increased sinus pauses in mice and man *in vivo*

To determine the impact of loss of DSP on cardiac conduction *in vivo*, we monitored cardiac rhythm in DSP csKO mice via ECG telemetry. Adult DSP csKO mice presented with a significant increase in the

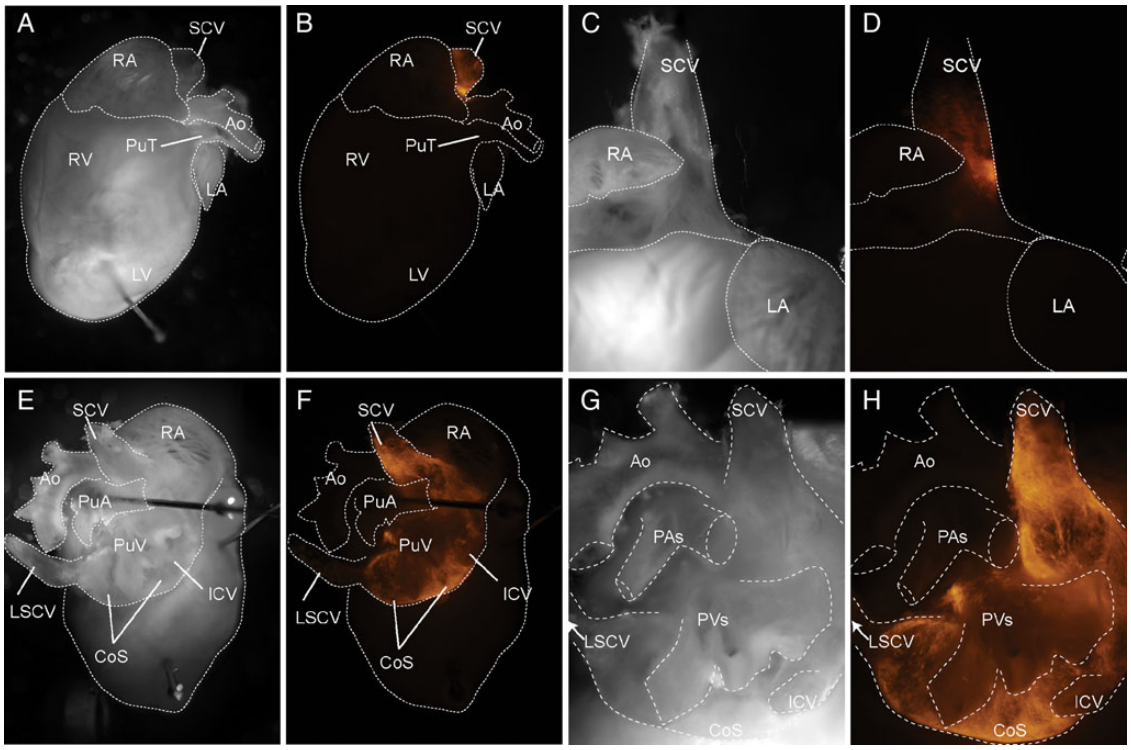


**Figure 2** Hcn4 promoter-driven Cre recombinase activity targets the adult mouse pacemaker complex. Representative whole mount pictures from a $Dsp^{flox/+}$:$Hcn4^{creERT2(+)}$: $ROSA26^{TomRed+}$ adult mouse after tamoxifen administration: Brightfield (*A, C, E,* and *G*) and TomRed fluorescence (*B, D, F,* and *H*). Anterior views (*A–D*) of the mouse heart show TomRed expression localized to the junction of the superior caval vein (SCV). Posterior views (*E–H*) highlight TomRed expression in a mesh-like network surrounding the large coronary sinus (CoS). RA, right atrium; Ao, aorta; PuT, pulmonary trunk; LA, left atrium; RV, right ventricle; LV, left ventricle; PuA, pulmonary artery; PuV, pulmonary vein; ICV, inferior caval vein; LSCV, left superior caval vein.

number of sinus pauses during periods of rest (*Figure 4A* and *B*). Sinus pauses were observed in the absence of cardiomyopathy as no significant differences in left ventricular dimensions and function (see Supplementary material online, *Table S1*), as well as atrial fibrosis (see Supplementary material online, *Figure S4*), could be observed between adult DSP csKO and control hearts.

We also show evidence from a clinical case that provides the first demonstration of a deleterious human DSP variant that primarily associates with a phenotype of sinus pause/bradycardia in the absence of cardiomyopathy (*Figure 4C–E*). A 19-year-old male presented with isolated ventricular ectopies (>40 000 in 24 h). He denied syncope or pre-fainting episodes and had a negative family history for sudden death and/or known cardiac disease. Clinical evaluation revealed marked sinus bradycardia (30–40 bpm) and frequent sinus pauses (*Figure 4C–E*). Cardiac MRI showed preserved global left (LV) and right (RV) ventricular systolic function (LV ejection fraction: 51%; RV ejection fraction: 46%) as well as the absence of focal wall motion abnormalities and scarring. No ventricular ectopies and/or sustained arrhythmias were elicited either at baseline or after isoproterenol infusion during an electrophysiological study (EPS). However, the EPS showed marked sinus dysfunction, with a sinus node recovery time (SNRT) of 3 s (cSNRT 1.5 s). Prolonged rhythm monitoring with Linq (Medtronic) loop recorder demonstrated the occurrence of frequent sinus pauses of ~3 s (*Figure 4E*). Comprehensive cardiomyopathy screening from a commercial panel, which included 77 genes revealed the presence of a heterozygous splice site mutation in the DSP gene [c273 + 5 G > A, IVS2 + 5 G > A]. This mutation has been previously reported in two paediatric cases diagnosed with ARVC, and it is expected to destroy a natural splice donor site at intron 2, which is predicted to cause abnormal gene splicing.[22,23] This DSP variant was absent in >500 healthy controls screened and not reported in the NHLBI Exome Sequencing Project (6500 healthy individuals of both Europe and African American ancestries). Cascade screening revealed the same DSP variant in the patient's mother (clinical evaluation pending, but no reported history or signs of cardiomyopathy are known for this individual).

## 3.4 Loss of DSP leads to loss of beat-to-beat regulation in mice *in vivo*

Even in the absence of sinus pauses, we also observed a scatter of inter-beat intervals (IBI) at periods of lower heart rates in DSP csKO mice compared with controls (*Figure 5A*). To determine whether the observed scatter was different between control and DSP csKO mice, we statistically assessed IBI variability during a 20-min interval, using SD of beat-to-beat intervals (SDNN) (*Figure 5B*), SD of the difference between intervals (SD of delta NN) (*Figure 5C*), and root mean square of the successive differences (RMSSD) (*Figure 5D*). All of these parameters were significantly increased in adult DSP csKO mice compared with control groups (*Figure 5B–D*). No significant differences in mean heart rates were observed between adult DSP csKO and control mice during this time frame (*Figure 5E*). Additionally, no significant

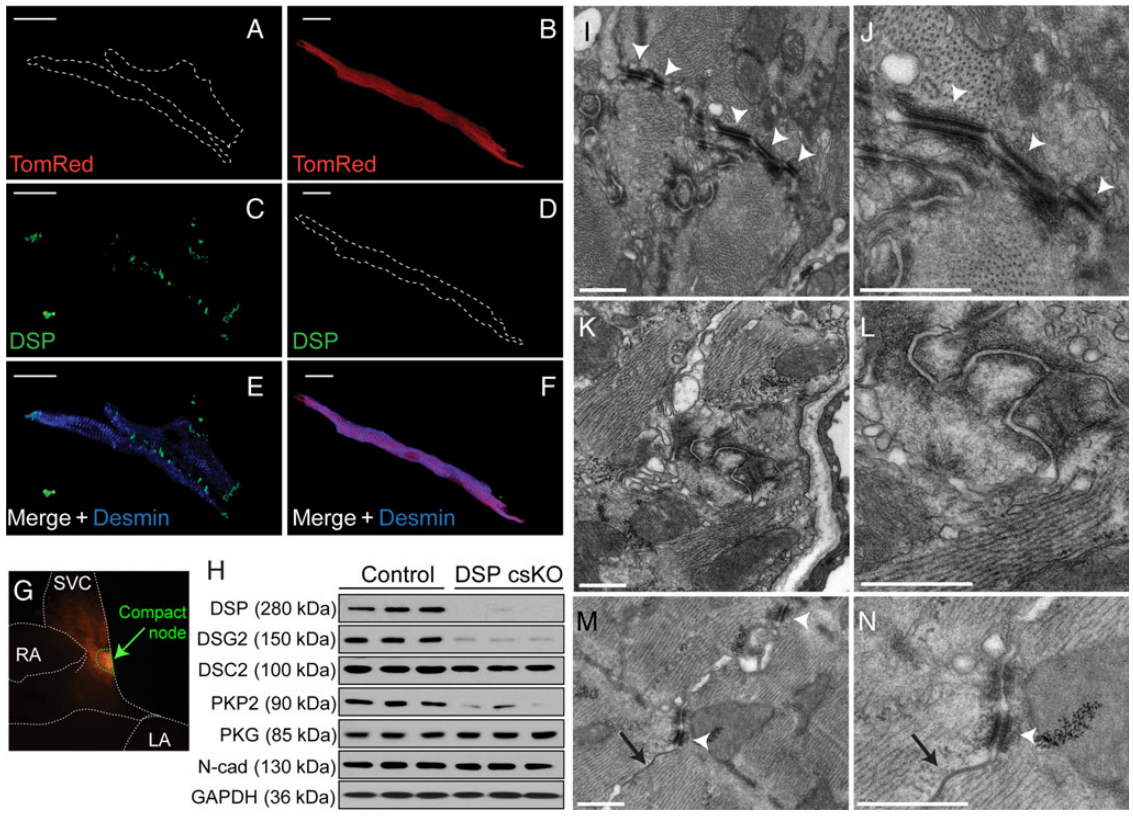


**Figure 3** DSP csKO pacemaker cells display loss of DSP protein and the absence of desmosomal structures. (*A*–*F*) IF staining of DSP in TomRed-negative and TomRed-positive pacemaker cardiomyocytes isolated from the SAN of a tamoxifen-injected DSP csKO mouse ($Dsp^{flox/flox}$:$Hcn4^{creERT2(+)}$:-$ROSA26^{TomRed+}$). Cells were double labelled with antibodies against (*C* and *D*) DSP (green) and (*E* and *F*) desmin (blue) as well as fluorescently imaged for (*A* and *B*) TomRed (red). Bars represent 20 μm. Cells were examined from five mouse hearts per genotype. (*G*) Representative epifluorescence image highlighting TomRed-positive compact node tissue (green dashed outline) that is observed in control ($Dsp^{flox/+}$:$Hcn4^{creERT2(+)}$:$ROSA26^{TomRed+}$) and DSP csKO ($Dsp^{flox/flox}$:$Hcn4^{creERT2(+)}$: $ROSA26^{TomRed+}$) mice and used for protein analysis. (*H*) Immunoblot analysis of desmosomal and fascia adherens junction proteins as well as GAPDH (loading control) from compact nodal tissue ($n = 3$ mice per genotype). DSP, desmoplakin; DSC2, desmocollin-2; DSG2, desmoglein-2; PKP2, plakophillin-2; PKG, plakoglobin; N-cad: N-cadherin. (*I*–*N*) Representative transmission electron micrographs from the pacemaker complex of (*I* and *J*) littermate control and (*K* and *L*) DSP csKO mice as well as (*M* and *N*) atrial muscle from the same tamoxifen-injected DSP csKO. Sections were examined from four mouse hearts per genotype. White arrowheads denote desmosomes. Black arrows denote gap junctions. Bars for *I*–*N* represent 500 nm.

differences in PR and QRS intervals could be observed in adult DSP csKO vs. control mice (see Supplementary material online, *Figures S5*).

## 3.5 Loss of DSP triggers loss of beat-by-beat regulation independent of autonomic influence

To dissect the effect of DSP loss on PC function in a system independent of autonomic or atrial volume load influence, we used an *ex vivo* SAN-right atrial preparation in which the tissue remains spontaneously depolarizing as previously described.[5] Electrodes were placed on the atrial tissue to assess IBI (*Figure 6A*). A representative graph of IBI from control and DSP csKO atria highlights the variability of consecutive intervals when DSP is lost from the PC (*Figure 6B*). Similar to *in vivo* findings, we show that mean IBI did not significantly differ between adult DSP csKO and control atria (*Figure 6C*); however, the coefficient of variation of IBI was significantly increased in adult DSP csKO vs. control atria (*Figure 6D*). These results show that beat-to-beat regulation is lost in a system independent of autonomic regulation or a response to stretch due to fluctuations in volume load.

## 3.6 Loss of DSP triggers defects in site of dominant mouse pacemaker localization, which is associated with loss of connexin 45 protein expression

To understand the mechanisms underlying the loss of rhythmicity associated with DSP loss, we evaluated P–P intervals and wave morphology as well as the earliest point (lead site) of SAN activation in the mouse atria. Representative tracings from controls revealed uniform depolarizations of the same morphology throughout successive beats, whereas DSP csKO atria revealed depolarizations of varying morphology throughout successive beats (*Figure 7A* and *B*). Optical maps of action potential propagation within mouse atria revealed that the earliest site of activation (dominant pacemaker) for controls was located at a single site in the PC (*Figure 7A*), while the lead pacemaker site was exclusively observed in DSP csKO atria to dynamically shift to a second site

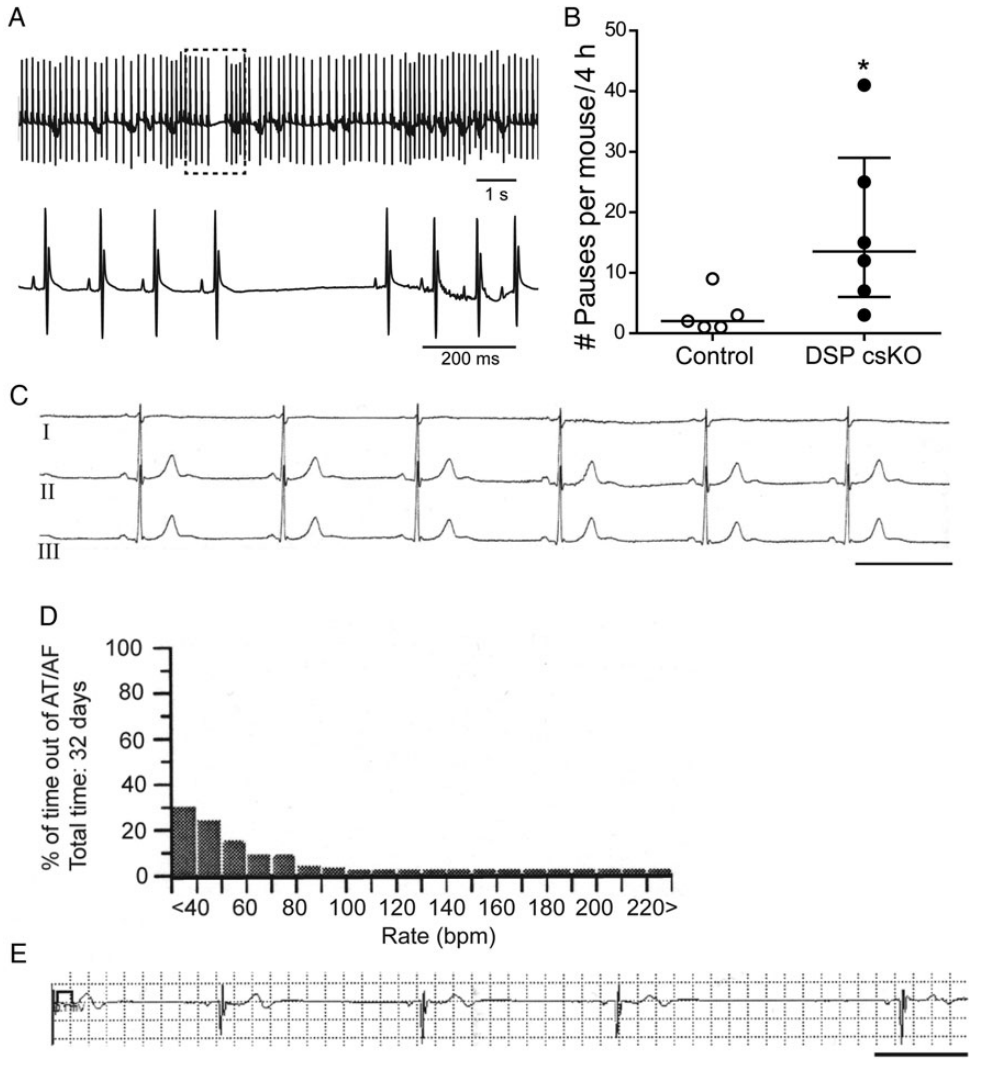


**Figure 4** Dysregulation of DSP (loss or mutation) leads to increased sinus pauses in mice and man *in vivo*. (*A*) Upper panel: Representative ECG telemetry trace from a DSP csKO mouse. Lower panel: Expanded view of sinus pause in hatched box. (*B*) Quantification of sinus pauses in a period of 4 h from DSP csKO and littermate control mice. Number of pauses observed from each individual mouse is graphed in circles. Open circles and open bar: Control mice; Closed circles and black bar: DSP csKO mice ($n = 5$ for control, $n = 6$ for DSP csKO). *$P < 0.05$. (*C*) Lead I–III ECG showing sinus bradycardia (38 bpm) in the 19-year-old patient carrier of the DSP mutation c273 + 5 G > A. Scale bar: 1 s. (*D*) Ventricular rate histogram from 32 days loop recorder monitoring showing sinus bradycardia with heart rate values <60 bpm for 70% of time. (*E*) ECG strip recorded by the implantable loop recorder (Medtronic Linq) showing a diurnal sinus pause of 3 s. Scale bar: 1 s.

between successive beats, coincident with altered P wave morphology (*Figure 7B*), highlighting a potential alteration in electrical communication across the PC. These data recapitulate independent *in vivo* observations of varying P wave morphology in telemetry ECG recordings from adult DSP csKO mice (*Figure 7C*).

To understand the mechanisms underlying the altered electrical communication within the PC in DSP csKO atria, we examined protein expression of connexin 45, a major molecular regulator of electrical coupling in the PC.[4,7,22] Previous studies have reported that desmosomal integrity is necessary to maintain gap junction expression and function in the working ventricular myocardium;[10,23] however, this connection has not been explored in cardiomyocytes of the PC. Protein blot analysis revealed that connexin 45 protein expression and localization is dramatically down-regulated in compact SAN and SAN cells from adult DSP csKO mice, compared with controls (*Figure 7D*; see Supplementary material online, *Figure S6*). No significant differences in connexin 45 transcript levels could be detected in compact SAN of adult DSP csKO vs. controls (see Supplementary material online, *Figure S6*), suggesting that the down-regulation of connexin 45 is at the post-transcriptional level. The loss of connexin45 protein expression in DSP csKO mice was also observed in the absence of changes in the expression of Hcn4 protein levels (*Figure 7D*), demonstrating that loss of DSP mechanistically impacts gap junction channel expression and function in the PC. These results further suggest that similar to other genetic models,[24,25] post-transcriptional compensatory mechanisms may play a major role in maintaining Hcn4 protein levels in the SAN of the haploinsufficient Hcn4-Cre mouse model. Interestingly, protein levels of connexin 43 and connexin 30.2, which are connexin isoforms also

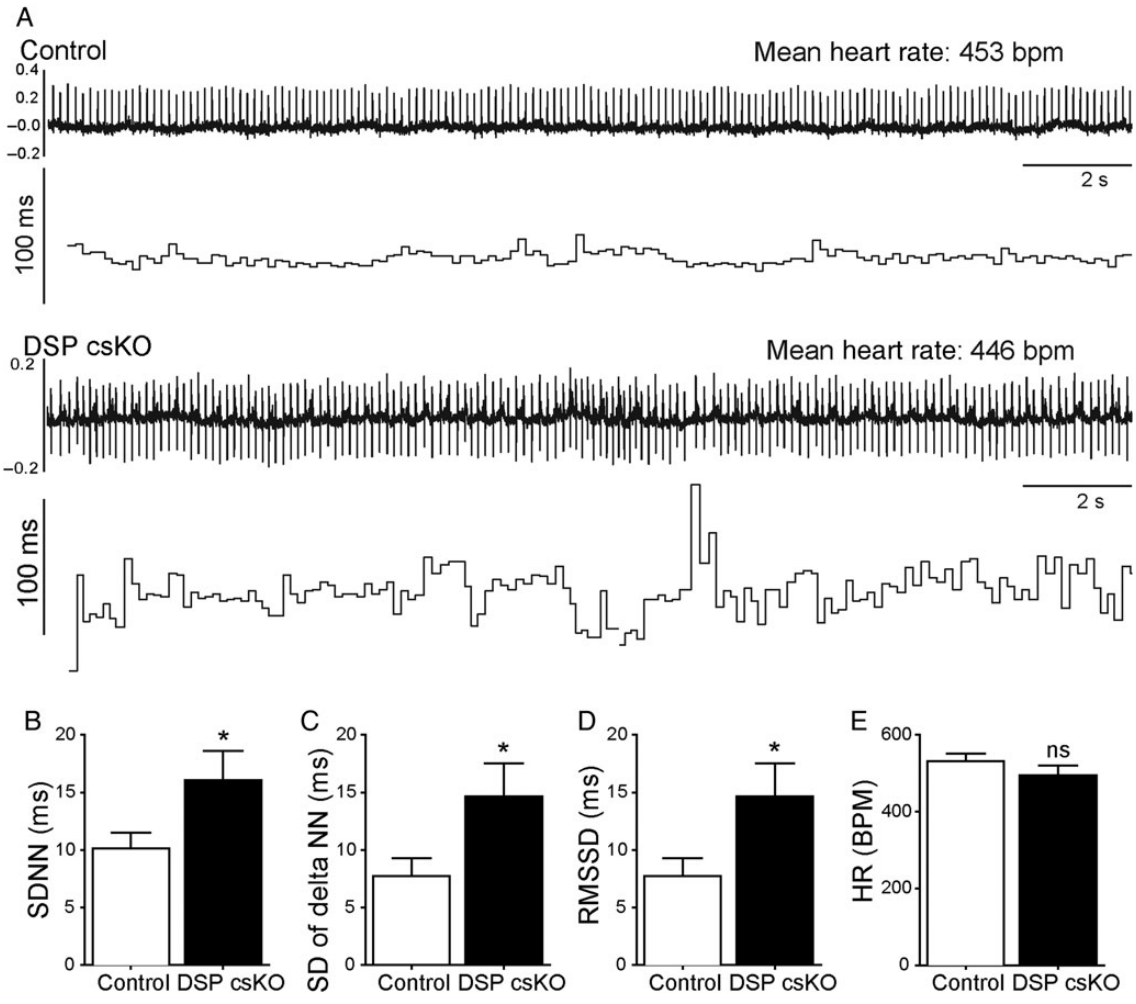


**Figure 5** DSP loss from the mouse PC leads to increased beat-by-beat regulation with no change in heart rate. (*A*) Representative ECG telemetry (upper trace) and R–R interval analysis (lower trace) obtained from control and DSP csKO mice. (*B–E*) Analysis of beat-to-beat variability in a 20 min period of ECG telemetry ($n = 9$ mice per genotype). (*B*) SD of RR intervals (SDNN), (*C*) SD of the difference between intervals (SD of delta NN), (*D*) root mean square of the successive differences (RMSSD), and (*E*) heart rates (bpm) from the period analysed. $^*P < 0.05$; ns, not significant.

expressed in the compact SAN,[26,27] were not significantly different in the compact SAN of adult DSP csKO mice vs. controls (*Figure 7D*). These results further demonstrate the specificity for connexin 45 protein loss in DSP-deficient SAN as well as show that compensatory mechanisms related to other connexin isoforms do not likely contribute to the SAN phenotype in DSP csKO mice.

## 3.7 Neonatal mouse ventricular cardiomyocytes harbouring DSP loss phenocopy the loss of beat-to-beat regulation in adult DSP csKO mice and atria

To determine whether the primary defects in beat-to-beat regulation due to DSP loss occur (i) independent of autonomic influence and (ii) prior to any consequences on loss of structural integrity of the cells that occurs with long-term ablation of DSP, we exploited DSP floxed neonatal ventricular cardiomyocytes (NMVC).[10] NMVC is a distinct cardiac cellular model system that also undergoes beat-to-beat regulation and displays spontaneous depolarization activity similar to pacemaker cells.[26] The DSP floxed NMVC model was also advantageous as it provides an independent system of isolating the effect of DSP deficiency on beat-to-beat variability in a network of spontaneously beating cells without the influence of extrinsic factors that might modify their pacemaking behaviour. We show that mean cycle lengths do not significantly differ between control vs. DSP-deficient NMVC (*Figure 8B*). However, IBI coefficient of variation is significantly increased in DSP-deficient NMVC compared with controls (*Figure 8C*). These effects occur prior to any structural loss in continuity within the cardiomyocyte monolayers, as evidenced by the retained localization and expression of the cell junction protein, plakoglobin (see Supplementary material online, *Figure S7*). However, our studies do not rule out the possibility that there could be other structural defects that are not apparent at the resolution of plakoglobin distribution (namely LM) that were not assessed in the NMVC model. Representative IBI analysis (*Figure 8A*) and optical maps of action potential propagation (see Supplementary material online, *Figure S8*) between DSP-deficient and control NMVC highlight the dispersion in beat-to-beat intervals in DSP-deficient cardiomyocytes, which phenocopy observations in DSP csKO mice and DSP csKO atria.

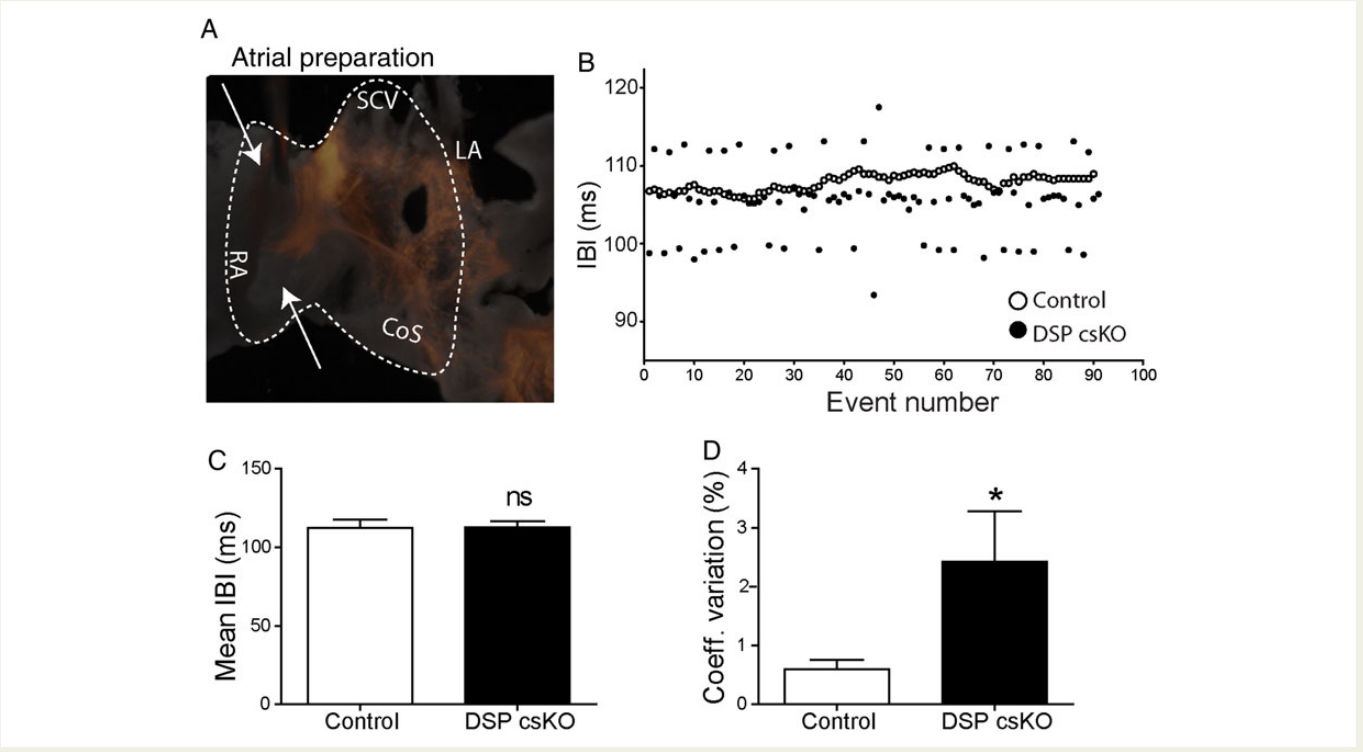


**Figure 6** DSP loss in mouse PC leads to loss of beat-by-beat regulation in mouse atria. (*A*) Representative image of an *ex vivo* atrial preparation used to evaluate interbeat interval (IBI) variability through high resolution optical mapping. Recording electrodes were placed in the regions indicated by arrows. Dotted region indicates the area acquired by the camera. (*B*) Representative tachogram of NN intervals (depicted as event numbers) from an adult littermate control (open circles) and DSP csKO (closed circles) mice atria. Quantification of (*C*) mean cycle length and (*D*) coefficient of variation of NN intervals in adult littermate control ($n = 9$) and DSP csKO atria ($n = 9$). *$P < 0.05$; ns, not significant.

## 4. Discussion

Current understanding of SAN function has focused on the electrophysiological and single-cell properties of pacemaker cells that give rise to an action potential. Research has primarily aimed at understanding rhythmic diastolic depolarizations that result from mutual entrainment of two cycling systems: funny current-driven membrane or voltage clock (M clock) and a calcium clock.[27] Structures responsible for coupling include well-established membrane ion channels, ion transporters, and calcium handling proteins.[3,27] However, more recently, it has been increasingly clear that despite the rudimentary contractile apparatus of the SAN, critical to the SAN cell–cell interface are intrinsic structural (anchoring) connections which include desmosomes,[7] whose role in the pacemaker remains unexplored.

Dysregulation of desmosomes (via mutations or loss-of-function studies) has been primarily associated with arrhythmogenic right ventricular cardiomyopathy (ARVC), thus establishing a dominant role for desmosomes, and, the central desmosomal component, desmoplakin in maintaining mechanical integrity of ventricular cardiomyocytes.[8] However, recent implications have suggested the potential importance for desmosomal proteins/structures in cells of the cardiac conduction system and sinus node;[28,29] yet their role has not been evaluated as a disease pathway for sinus node dysfunction. The severe cardiac phenotype in previous cardiomyocyte-specific DSP-deficient models[10,30] using cardiomyocyte Cre drivers that can also target cardiac conduction cells[31,32] has precluded the ability to study pacemaker-specific defects in these models, independent of secondary influences from working (ventricular) cardiomyocytes. By exploiting an inducible *Hcn4-Cre-ER*$^{T2}$ mouse line, we reveal an essential and specific role for desmoplakin and desmosomal junctions in adult SAN function and lead pacemaker cells, which showed the most vulnerability to loss of desmoplakin and disruption of desmosomes. Thus, these studies further validate the potential utility of *Hcn4-Cre-ER*$^{T2}$ mouse line as a valuable model system for cardiac conduction (pacemaker) restricted gene targeting.

We provide functional relevance to studies that show the presence of desmosomes in the SAN[18,19] (*Figure 1*), as well as provide important contextual insights into the hierarchy of proteins that are functionally relevant to SAN junctions. We highlight the specificity of the junctional defects resulting from DSP loss in the SAN, which exclusively targets desmosomal but not the fascia adherens proteins. The compartmentalized nature of desmosomal protein loss in DSP-deficient SAN suggests a model of compartmentalized vs. mixed (desmosomal vs. fascia adherens) anchoring junctions in the SAN as no compensation from fascia adherens junction proteins was observed. Thus, lack of a major role for desmosomes in other cardiac conduction structures (AV node and His-Purkinje) may be partly due to the distinct cellular architecture and protein hierarchy that make up the anchoring junctions in different conduction system structures. In ventricular conduction structures (Purkinje fibres),[14] it has been established that mixed hybrid adherens junctions (combination of desmosome and fascia adherens junction) prevail, which further reinforce the prominent sarcomeric and cytoskeletal architecture of the ventricular muscle. These mixed junctions have not been reported in SAN cardiomyocytes, which is indirectly

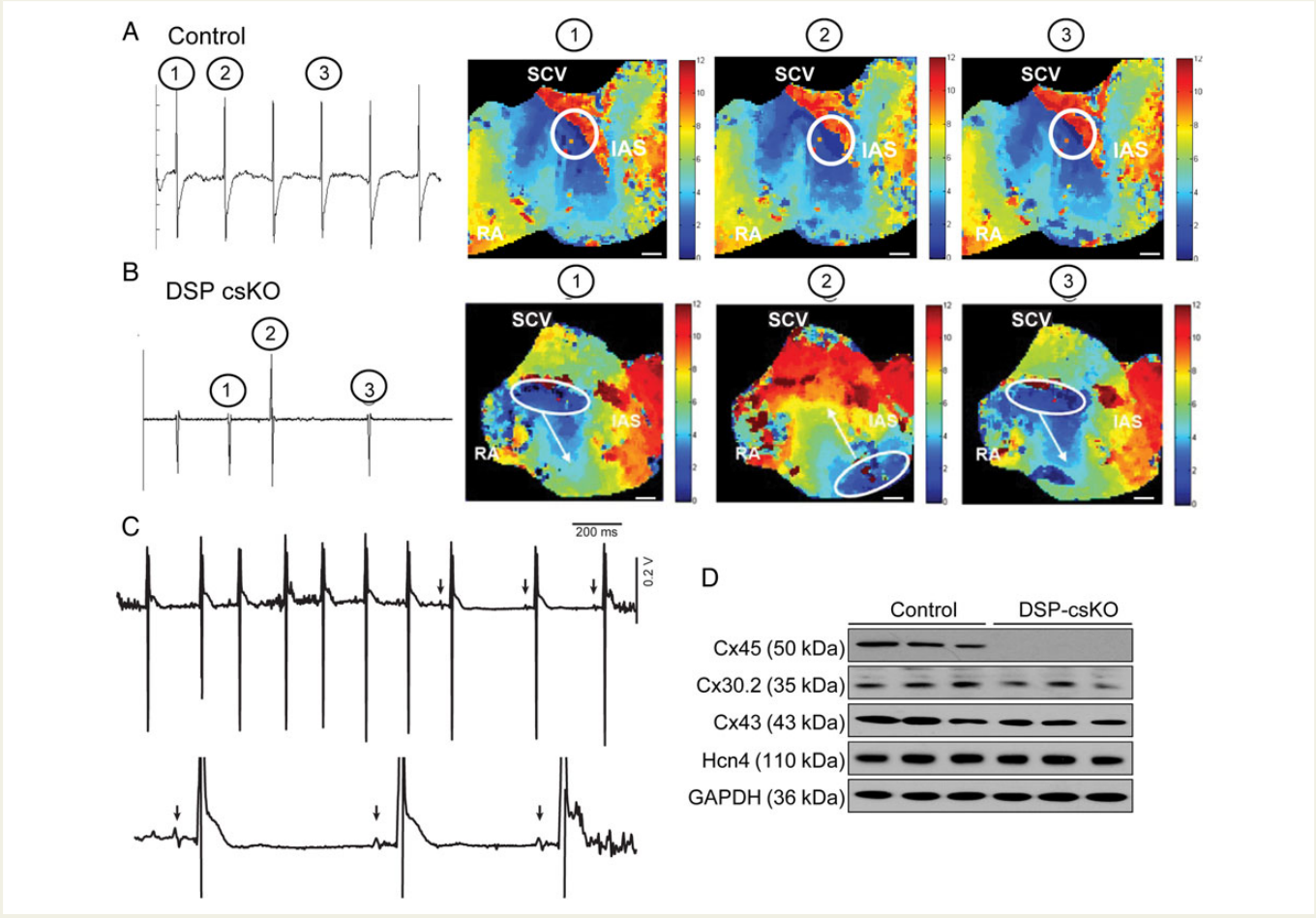


**Figure 7** DSP loss in mouse PC leads to beat-by-beat shifts in lead pacemaker site, which is associated with connexin 45 protein loss. (*A*–*B*) Representative electrograms and action potential propagation maps from a control (*A*) and a DSP csKO (*B*) mouse. A propagation maps were evaluated from five mice per genotype. A representative map shows the site of initial depolarization (white circle) for the corresponding electrogram action potentials, which are depicted as encircled numbers: 1, 2, and 3. White bar = 1 mm. (*C*) Representative ECG trace obtained from a DSP csKO mouse showing the changes in P wave morphology that occurs *in vivo*. This phenomenon was observed in all DSP csKO mice examined in this study ($n = 8$). (*D*) Protein blot analysis of connexin 45, connexin 30.2, connexin 43, and HCN4 expression in compact node tissue lysates from adult DSP csKO and littermate control mice. GAPDH was used as a loading control. The blots were evaluated from three mice per genotype.

supported by our above findings. Thus, fascia adherens junction proteins may compensate for the loss of desmosomal proteins in these mixed junctions found between Purkinje fibres but not in the SAN.

Current mouse models have attributed the direct loss of ion channels and ion channel regulators as key factors in the development of pacemaker dysfunction, some of which alter heart rate.[3,33–36] However, we shed new light on pacemaker biology to reveal the importance of desmosomal junctions between pacemaker cells in the baseline regulation of mouse SAN function in the adult heart. In the absence of autonomic stimuli (*ex vivo* atrial preparations), the loss of desmosomal integrity leads to a loss of communication between different pacemaker foci resulting in beat-to-beat migration of the lead pacemaker that may underlie the IBI variability observed in DSP csKO mice *in vivo*. These studies suggest that mutual entrainment of pacemaker cells requires desmosomes, and that loss of anchorage between these cells may be a contributing factor to sinus node disease by precluding electrical communication between SAN cells. Importantly, we suggest a mechanism for sinus pauses not due to atrial block (no evidence of Mobitz II or Wenckebach conduction) or sinus arrest (mean heart rates and cycle lengths of isolated atria are not significantly different from control mice) but due to loss of desmosomal junctions between pacemaker cells. We also suggest that desmosomes are integral for electrical coordination between pacemaker cells, which may be an underlying mechanism for the sinus pauses *in vivo*. Interestingly, our studies may add a new level of complexity to interpretations related to heart rate variability *in vivo*, which we show can be independent of vagal tone (autonomic stimulation), as shown in studies done in DSP csKO atria *ex vivo* and DSP-deficient cardiomyocytes *in vitro*.

In contrast to the working myocardium, coupling in the mouse PC mainly occurs through low conductance gap junctions formed by connexin 45, 30.2, and 30.[4,7,22,37] Computer simulations and *ex vivo* studies were the first to provide evidence to the notion that loss of gap junction communication may result in loss of mutual entrainment;[6,38] however, little is known about the relevance of pacemaker entrainment and their underlying mechanisms *in vivo*. Our studies show that loss of DSP leads to a concurrent specific loss of connexin 45 protein levels and localization in the SAN, which was associated with a physiological disruption in lead pacemaker communication. The down-regulation of

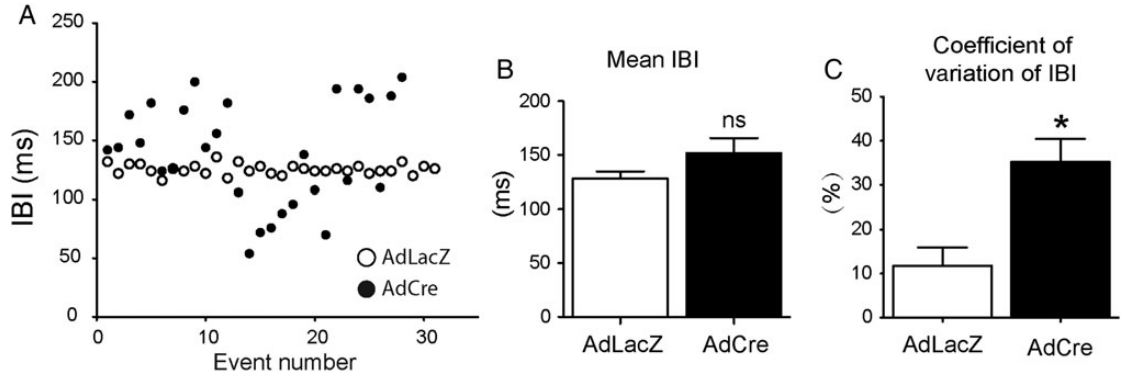


**Figure 8** DSP loss in neonatal mouse ventricular cardiomyocytes elicits loss of beat-by-beat regulation *in vitro*. (*A*) Representative analysis of intervals between consecutive depolarizations in DSP-deficient (AdCre) and control (AdLacZ) nenonatal mouse ventricular cardiomyocyte cultures, with each data point represented on the graph. Quantification of (*B*) mean cycle length and (*C*) IBI coefficient of variation in AdLacZ (control) and AdCre (DSP deficient) cardiomyocytes. $n = 3$ represents three independent experiments, where each experiment represents cardiomyocytes isolated from a pool of 8–10 neonatal DSP floxed mice (one litter) and plated in triplicate for each condition. $^*P < 0.05$; ns, not significant.

connexin 45 was found to occur at the post-transcriptional level. Although the mechanisms underlying this dysregulation remain to be understood, recent evidence highlights the cardiac cell–cell junction as an active site of protein degradation,[39] suggesting a potential mechanism whereby dysregulation of desmosomal junctions could potentially trigger dysregulation of protein degradation mechanisms at this site, which could then impact connexin protein levels. Functionally, the decrease in connexin 45 protein levels could also physiologically explain multiple lead pacemakers losing entrainment and depolarizing at different beating rates. We believe the mechanism of increased variability found in SAN also extend to working (ventricular) cardiomyocytes, as we showed loss of beat-to-beat regulation in DSP-deficient ventricular cardiomyocytes. This is in a system and time point where we previously observed early loss of connexin 43,[10] the connexin 45 counterpart in working (ventricular) cardiomyocytes. These studies are in contrast to mouse models where ablation of the anchoring junction protein coxsackie adenovirus receptor in cardiomyocytes resulted in AV block and selective loss of connexin 45 within the atrioventricular node,[31,40] further highlighting that there may be a distinct hierarchy of cell–cell junction proteins in SAN vs. other conduction structures. Although desmosomal proteins are thought to be important for ion channel stability or biophysical properties,[12,13] it remains to be determined in the future whether specific ion channels, particularly those that form part of the membrane clock, are in close proximity to desmosomes in the SAN and whether their disruption could affect channel biology.

Pathophysiological stresses such as hypertension, heart failure, and oxidative stress are all thought to contribute to sinus node dysfunction and disease.[41–43] Recent studies highlight that secondary effects associated with sinus node dysfunction and disease may account for sudden death in a large portion of patients hospitalized with heart failure[44–46] and may also be a better predictor of mortality in heart failure patients, when compared with ventricular arrhythmias.[47] Our studies provide new insights into mechanisms underlying SAN dysfunction, by demonstrating that dysregulation of desmosomal junctions in the SAN have a primary effect on adult SAN function. This is relevant in this context, as remodelling of desmosomal junctions has been observed in an animal model of mechanical pressure overload,[48] further highlighting a link for desmosomes in mechanotransduction pathways. These findings may also have direct importance to humans as we provide to our knowledge the first report of a patient harbouring a deleterious DSP variant that associates primarily with a phenotype of sinus bradycardia and pauses in the absence of signs of cardiomyopathy. Although it could be argued that the overt cardiomyopathy phenotype could progressively develop in the future as this variant has been reported in paediatric cases of ARVC,[22,23] the first clinical manifestation leading to the diagnosis in our patient was purely related to sinus node dysfunction. This case adds to growing case reports that demonstrate pacemaker dysfunction and in some cases, specifically sinus pauses, in ARVC patients.[49–52] These studies altogether highlight an essential role for desmosomal integrity in human PC function and may point in some cases to signs of early disease manifestation in the concealed phase of ARVC. Although further work is needed in this area, these data suggest that strategies focused on reinforcing desmosomes in the SAN may provide an approach to circumventing SAN dysfunction in these patients.

Studies have also attributed fibrosis as a major factor contributing to pacemaker dysfunction.[38,53] The SAN is thought to undergo age-related changes both in structure and in function (degree of electrical coupling is thought to decrease with age).[54] Some studies have implicated that fibrosis contributes to this age-related remodelling; however, these assumptions remain controversial.[55] In light of our findings, studies directed at determining whether desmosomal alterations contribute to age-related SAN remodelling and/or exacerbate the arrhythmia landscape in the ageing heart are important and warranted for the future.

Our studies provide evidence of a novel mechanism that can further our understanding of SAN physiology and function as an emergent property of a network of pacemaker cells that require desmosomal junctions for synchronous function. This has broad implications in understanding mechanisms underlying beat-to-beat regulation as well as underlying sinus node disease and dysfunction. We believe these studies also provide a novel basis to move the field beyond the ionic properties of isolated SAN cells towards a better understanding of a co-ordinated network that is capable of integrating complex structural information at the tissue level.

# Supplementary material

Supplementary material is available at *Cardiovascular Research* online.

## Acknowledgements

We thank the Farquhar Laboratory Transmission Electron Microscopy Core Facility (UCSD, La Jolla, CA) for technical assistance with electron microscopy. Microscopy work was performed at the University of California, San Diego Neuroscience Microscopy Shared Facility.

**Conflict of interest:** none declared.

## Funding

The University of California San Diego Neuroscience Microscopy Shared Facility is supported by a grant from the National Institutes of Health (P30 NS04710). Optical mapping studies were supported in part by NIH grants from NHLBI and NIGMS to A.D.M.; R.C.L. was a recipient of an American Heart Association Postdoctoral Fellowship. R.C.L. is currently supported by a NIH T32 training grant. F.S. is supported by grants from NIH/NHLBI, Saving tiny Heart Society, American Heart Association, California Institute of Regenerative Medicine and Tobacco Related Disease Research Program.

## References

1. Boyett MR, Dobrzynski H. The sinoatrial node is still setting the pace 100 years after its discovery. *Circ Res* 2007;**100**:1543–1545.
2. Jalife J. Mutual entrainment and electrical coupling as mechanisms for synchronous firing of rabbit sino-atrial pace-maker cells. *J Physiol* 1984;**356**:221–243.
3. Mangoni ME, Nargeot J. Genesis and regulation of the heart automaticity. *Physiol Rev* 2008;**88**:919–982.
4. Boyett MR, Honjo H, Kodama I. The sinoatrial node, a heterogeneous pacemaker structure. *Cardiovasc Res* 2000;**47**:658–687.
5. Glukhov AV, Fedorov VV, Anderson ME, Mohler PJ, Efimov IR. Functional anatomy of the murine sinus node: high-resolution optical mapping of ankyrin-B heterozygous mice. *Am J Physiol Heart Circ Physiol* 2010;**299**:H482–H491.
6. Delmar M, Jalife J, Michaels DC. Effects of changes in excitability and intercellular coupling on synchronization in the rabbit sino-atrial node. *J Physiol* 1986;**370**:127–150.
7. Mezzano V, Pellman J, Sheikh F. Cell junctions in the specialized conduction system of the heart. *Cell Commun Adhes* 2014;**21**:149–159.
8. Sheikh F, Ross RS, Chen J. Cell-cell connection to cardiac disease. *Trends Cardiovasc Med* 2009;**19**:182–190.
9. Vasioukhin V, Bowers E, Bauer C, Degenstein L, Fuchs E. Desmoplakin is essential in epidermal sheet formation. *Nat Cell Biol* 2001;**3**:1076–1085.
10. Lyon RC, Mezzano V, Wright AT, Pfeiffer E, Chuang J, Banares K, Castaneda A, Ouyang K, Cui L, Contu R, Gu Y, Evans SM, Omens JH, Peterson KL, McCulloch AD, Sheikh F. Connexin defects underlie arrhythmogenic right ventricular cardiomyopathy in a novel mouse model. *Hum Mol Genet* 2014;**23**:1134–1150.
11. Gomes J, Finlay M, Ahmed AK, Ciaccio EJ, Asimaki A, Saffitz JE, Quarta G, Nobles M, Syrris P, Chaubey S, McKenna WJ, Tinker A, Lambiase PD. Electrophysiological abnormalities precede overt structural changes in arrhythmogenic right ventricular cardiomyopathy due to mutations in desmoplakin-A combined murine and human study. *Eur Heart J* 2012;**33**:1942–1953.
12. Sato PY, Musa H, Coombs W, Guerrero-Serna G, Patino GA, Taffet SM, Isom LL, Delmar M. Loss of plakophilin-2 expression leads to decreased sodium current and slower conduction velocity in cultured cardiac myocytes. *Circ Res* 2009;**105**:523–526.
13. Cerrone M, Noorman M, Lin X, Chkourko H, Liang FX, van der Nagel R, Hund T, Birchmeier W, Mohler P, van Veen TA, van Rijen HV, Delmar M. Sodium current deficit and arrhythmogenesis in a murine model of plakophilin-2 haploinsufficiency. *Cardiovasc Res* 2012;**95**:460–468.
14. Pieperhoff S, Borrmann C, Grund C, Barth M, Rizzo S, Franke WW. The area composita of adhering junctions connecting heart muscle cells of vertebrates. VII. The different types of lateral junctions between the special cardiomyocytes of the conduction system of ovine and bovine hearts. *Eur J Cell Biol* 2010;**89**:365–378.
15. Bang ML, Li X, Littlefield R, Bremner S, Thor A, Knowlton KU, Lieber RL, Chen J. Nebulin-deficient mice exhibit shorter thin filament lengths and reduced contractile function in skeletal muscle. *J Cell Biol* 2006;**173**:905–916.
16. Liao Z, Lockhead D, Larson ED, Proenza C. Phosphorylation and modulation of hyperpolarization-activated HCN4 channels by protein kinase A in the mouse sinoatrial node. *J Gen Physiol* 2010;**136**:247–258.
17. Zemljic-Harpf AE, Miller JC, Henderson SA, Wright AT, Manso AM, Elsherif L, Dalton ND, Thor AK, Perkins GA, McCulloch AD, Ross RS. Cardiac-myocyte-specific excision of the vinculin gene disrupts cellular junctions, causing sudden death or dilated cardiomyopathy. *Mol Cell Biol* 2007;**27**:7522–7537.
18. Shimada T, Kawazato H, Yasuda A, Ono N, Sueda K. Cytoarchitecture and intercalated disks of the working myocardium and the conduction system in the mammalian heart. *Anat Rec A Discov Mol Cell Evol Biol* 2004;**280**:940–951.
19. Dobrzynski H, Rothery SM, Marples DD, Coppen SR, Takagishi Y, Honjo H, Tamkun MM, Henderson Z, Kodama I, Severs NJ, Boyett MR. Presence of the Kv1.5 K(+) channel in the sinoatrial node. *J Histochem Cytochem* 2000;**48**:769–780.
20. Bleeker WK, Mackaay AJ, Masson-Pevet M, Bouman LN, Becker AE. Functional and morphological organization of the rabbit sinus node. *Circ Res* 1980;**46**:11–22.
21. Opthof T, de Jonge B, Masson-Pevet M, Jongsma HJ, Bouman LN. Functional and morphological organization of the cat sinoatrial node. *J Mol Cell Cardiol* 1986;**18**:1015–1031.
22. Jansen JA, van Veen TA, de Bakker JM, van Rijen HV. Cardiac connexins and impulse propagation. *J Mol Cell Cardiol* 2010;**48**:76–82.
23. Sato PY, Coombs W, Lin X, Nekrasova O, Green KJ, Isom LL, Taffet SM, Delmar M. Interactions between ankyrin-G, Plakophilin-2, and Connexin43 at the cardiac intercalated disc. *Circ Res* 2011;**109**:193–201.
24. Minamisawa S, Gu Y, Ross J Jr., Chien KR, Chen J. A post-transcriptional compensatory pathway in heterozygous ventricular myosin light chain 2-deficient mice results in lack of gene dosage effect during normal cardiac growth or hypertrophy. *J Biol Chem* 1999;**274**:10066–10070.
25. Blanchard EM, Iizuka K, Christe M, Conner DA, Geisterfer-Lowrance A, Schoen FJ, Maughan DW, Seidman CE, Seidman JG. Targeted ablation of the murine alpha-tropomyosin gene. *Circ Res* 1997;**81**:1005–1010.
26. Rook MB, de Jonge B, Jongsma HJ, Masson-Pevet MA. Gap junction formation and functional interaction between neonatal rat cardiocytes in culture: a correlative physiological and ultrastructural study. *J Membr Biol* 1990;**118**:179–192.
27. Lakatta EG, Maltsev VA, Vinogradova TM. A coupled SYSTEM of intracellular Ca2+ clocks and surface membrane voltage clocks controls the timekeeping mechanism of the heart's pacemaker. *Circ Res* 2010;**106**:659–673.
28. Mezzano V, Sheikh F. Cell-cell junction remodeling in the heart: possible role in cardiac conduction system function and arrhythmias? *Life Sci* 2012;**90**:313–321.
29. Pieperhoff S. Gene mutations resulting in the development of ARVC/D could affect cells of the cardiac conduction system. *Front Physiol* 2012;**3**:22.
30. Garcia-Gras E, Lombardi R, Giocondo MJ, Willerson JT, Schneider MD, Khoury DS, Marian AJ. Suppression of canonical Wnt/beta-catenin signaling by nuclear plakoglobin recapitulates phenotype of arrhythmogenic right ventricular cardiomyopathy. *J Clin Invest* 2006;**116**:2012–2021.
31. Lim BK, Xiong D, Dorner A, Youn TJ, Yung A, Liu TI, Gu Y, Dalton ND, Wright AT, Evans SM, Chen J, Peterson KL, McCulloch AD, Yajima T, Knowlton KU. Coxsackievirus and adenovirus receptor (CAR) mediates atrioventricular-node function and connexin 45 localization in the murine heart. *J Clin Invest* 2008;**118**:2758–2770.
32. Pashmforoush M, Lu JT, Chen H, Amand TS, Kondo R, Pradervand S, Evans SM, Clark B, Feramisco JR, Giles W, Ho SY, Benson DW, Silberbach M, Shou W, Chien KR. Nkx2-5 pathways and congenital heart disease; loss of ventricular myocyte lineage specification leads to progressive cardiomyopathy and complete heart block. *Cell* 2004;**117**:373–386.
33. Ludwig A, Budde T, Stieber J, Moosmang S, Wahl C, Holthoff K, Langebartels A, Wotjak C, Munsch T, Zong X, Feil S, Feil R, Lancel M, Chien KR, Konnerth A, Pape HC, Biel M, Hofmann F. Absence epilepsy and sinus dysrhythmia in mice lacking the pacemaker channel HCN2. *EMBO J* 2003;**22**:216–224.
34. Baruscotti M, Bucchi A, Viscomi C, Mandelli G, Consalez G, Gnecchi-Rusconi T, Montano N, Casali KR, Micheloni S, Barbuti A, DiFrancesco D. Deep bradycardia and heart block caused by inducible cardiac-specific knockout of the pacemaker channel gene Hcn4. *Proc Natl Acad Sci USA* 2011;**108**:1705–1710.
35. Fenske S, Krause SC, Hassan SI, Becirovic E, Auer F, Bernard R, Kupatt C, Lange P, Ziegler T, Wotjak CT, Zhang H, Hammelmann V, Paparizos C, Biel M, Wahl-Schott CA. Sick sinus syndrome in HCN1-deficient mice. *Circulation* 2013;**128**:2585–2594.
36. Hao X, Zhang Y, Zhang X, Nirmalan M, Davies L, Konstantinou D, Yin F, Dobrzynski H, Wang X, Grace A, Zhang H, Boyett M, Huang CL, Lei M. TGF-beta1-mediated fibrosis and ion channel remodeling are key mechanisms in producing the sinus node dysfunction associated with SCN5A deficiency and aging. *Circ Arrhythm Electrophysiol* 2011;**4**:397–406.
37. Kreuzberg MM, Willecke K, Bukauskas FF. Connexin-mediated cardiac impulse propagation: connexin 30.2 slows atrioventricular conduction in mouse heart. *Trends Cardiovasc Med* 2006;**16**:266–272.
38. Lewis TJ, Rinzel J. Self-organized synchronous oscillations in a network of excitable cells coupled by gap junctions. *Network* 2000;**11**:299–320.
39. Lyon RC, Lange S, Sheikh F. Breaking down protein degradation mechanisms in cardiac muscle. *Trends Mol Med* 2013;**19**:239–249.
40. Lisewski U, Shi Y, Wrackmeyer U, Fischer R, Chen C, Schirdewan A, Juttner R, Rathjen F, Poller W, Radke MH, Gotthardt M. The tight junction protein CAR regulates cardiac conduction and cell-cell communication. *J Exp Med* 2008;**205**:2369–2379.
41. Swaminathan PD, Purohit A, Soni S, Voigt N, Singh MV, Glukhov AV, Gao Z, He BJ, Luczak ED, Joiner ML, Kutschke W, Yang J, Donahue JK, Weiss RM, Grumbach IM, Ogawa M, Chen PS, Efimov I, Dobrev D, Mohler PJ, Hund TJ, Anderson ME. Oxidized

CaMKII causes cardiac sinus node dysfunction in mice. *J Clin Invest* 2011;**121**:3277–3288.
42. Sanders P, Kistler PM, Morton JB, Spence SJ, Kalman JM. Remodeling of sinus node function in patients with congestive heart failure: reduction in sinus node reserve. *Circulation* 2004;**110**:897–903.
43. Opthof T, Coronel R, Rademaker HM, Vermeulen JT, Wilms-Schopman FJ, Janse MJ. Changes in sinus node function in a rabbit model of heart failure with ventricular arrhythmias and sudden death. *Circulation* 2000;**101**:2975–2980.
44. Uretsky BF, Sheahan RG. Primary prevention of sudden cardiac death in heart failure: will the solution be shocking? *J Am Coll Cardiol* 1997;**30**:1589–1597.
45. Stevenson WG, Stevenson LW, Middlekauff HR, Saxon LA. Sudden death prevention in patients with advanced ventricular dysfunction. *Circulation* 1993;**88**:2953–2961.
46. Faggiano P, d'Aloia A, Gualeni A, Gardini A, Giordano A. Mechanisms and immediate outcome of in-hospital cardiac arrest in patients with advanced heart failure secondary to ischemic or idiopathic dilated cardiomyopathy. *Am J Cardiol* 2001;**87**:655–657. A610-651.
47. Bloch Thomsen PE, Jons C, Raatikainen MJ, Moerch Joergensen R, Hartikainen J, Virtanen V, Boland J, Anttonen O, Gang UJ, Hoest N, Boersma LV, Platou ES, Becker D, Messier MD, Huikuri HV. Long-term recording of cardiac arrhythmias with an implantable cardiac monitor in patients with reduced ejection fraction after acute myocardial infarction: the Cardiac Arrhythmias and Risk Stratification After Acute Myocardial Infarction (CARISMA) study. *Circulation* 2010;**122**:1258–1264.
48. Chkourko HS, Guerrero-Serna G, Lin X, Darwish N, Pohlmann JR, Cook KE, Martens JR, Rothenberg E, Musa H, Delmar M. Remodeling of mechanical junctions and of microtubule-associated proteins accompany cardiac connexin43 lateralization. *Heart Rhythm* 2012;**9**:1133–1140. e1136.
49. Takemura N, Kono K, Tadokoro K, Shinbo G, Ito I, Abe C, Matsuhashi N, Iemura T, Nishikimi T, Horinaka S, Matsuoka H. Right atrial abnormalities in a patient with arrhythmogenic right ventricular cardiomyopathy without ventricular tachycardia. *J Cardiol* 2008;**51**:205–209.
50. Balderramo DC, Caeiro AA. Arrhythmogenic right ventricular dysplasia and sick sinus syndrome. *Medicina (B Aires)* 2004;**64**:439–441.
51. Nogami A, Adachi S, Nitta J, Taniguchi K, Marumo F, Aonuma K, Iesaka Y, Hiroe M. Arrhythmogenic right ventricular dysplasia with sick sinus syndrome and atrioventricular conduction disturbance. *Jpn Heart J* 1990;**31**:417–423.
52. Morady F, Shen EN, Scheinman MM. Unusual features of arrhythmogenic right ventricular dysplasia. *Am J Cardiol* 1984;**53**:639–640.
53. Herrmann S, Fabritz L, Layh B, Kirchhof P, Ludwig A. Insights into sick sinus syndrome from an inducible mouse model. *Cardiovasc Res* 2011;**90**:38–48.
54. Haqqani HM, Kalman JM. Aging and sinoatrial node dysfunction: musings on the not-so-funny side. *Circulation* 2007;**115**:1178–1179.
55. Jones SA. Ageing to arrhythmias: conundrums of connections in the ageing heart. *J Pharm Pharmacol* 2006;**58**:1571–1576.